Korean J. Chem. Eng., **28**(3), 800-807 (2011)
DOI: 10.1007/s11814-010-0426-x

Removal of methylene blue from aqueous solutions by adsorption onto chemically activated halloysite nanotubes

Peng Luo, Bing Zhang†, Yafei Zhao, Jinhua Wang, Haoqin Zhang, and Jindun Liu

School of Chemical Engineering, Zhengzhou University, Zhengzhou 450001, P. R. China
(*Received 22 February 2010 • accepted 7 September 2010*)

Abstract−This study examines the adsorption behavior of methylene blue (MB) from aqueous solutions onto chemically activated halloysite nanotubes. Adsorption of MB depends greatly on the adsorbent dose, pH, initial concentration, temperature and contact time. The Langmuir and Freundlich models were applied to describe the equilibrium isotherms and the Langmuir model agrees very well with experimental data. The maximum adsorption capacities for MB ranged from 91.32 to 103.63 $mg \cdot g^{-1}$ between 298 and 318 K. A comparison of kinetic models applied to the adsorption data was evaluated for pseudo-first-order, pseudo-second-order, Elovich and intra-particle diffusion equation. The results showed the adsorption process was well described by the pseudo-second-order and intra-particle diffusion mode. Thermodynamic parameters suggest that the adsorption is spontaneous and endothermic. The obtained results indicated that the product had the potential to be utilized as low-cost and effective alternative for dye removal in wastewater.

Key words: Halloysite Nanotubes, Adsorption, Methylene Blue, Isotherm, Kinetic Model

INTRODUCTION

Colored effluents are widely produced in industries such as textiles, leather, rubber, dye synthesis, printing, pulp mills, and food and plastics. Nowadays, their excessive release into the ecosystem represents increasing environmental problem due to their toxicity, mutagenicity, non-biodegradability and undesirable aesthetic aspects. The decolorization of dye effluents has received increasing attention, and thus various chemical, physical, physicochemical and biological treatment methods have been developed for the removal of dyes from aqueous solutions, such as adsorption, chemical/electrochemical coagulation, oxidation, filtration, membrane process and anaerobic/aerobic digestion [1-4].

Among these methods, adsorption has proven to be an effective and attractive treatment methodology with great potential applications. Generally, cost effectiveness, locally availability and adsorptive property are the main criteria for choosing an adsorbent. Currently, activated carbon [5-7], the most widely used adsorbent for dyes removal, has the disadvantages of high costs and problems associated with its subsequent treatment and regeneration. These limitations have encouraged the searches for inexpensive and readily available materials as adsorbents for dyes removal. A variety of unconventional materials including clay mineral, biomass, resin and solid waste are employed as adsorbents to remove dyes from colored wastewater [1,8-15]. Among them, clay minerals have been reported to be promising adsorbents due to their large specific surface area, cheap and abundant resources. Furthermore, the regeneration of these low-cost substitutes is not necessary, whereas regeneration of activated carbon is essential. Varied clays, such as kaolinite [16], bentonite [11,17], sepiolite [18], perlite [19], nontronite [20] and diatomite [21], have been tested for their ability of dye adsorption. However, taking local availability for various regions into consideration, new, economical and highly effective dye adsorbents are still needed.

Halloysite is a two-layered aluminosilicate clay mineral, consisting of one alumina octahedron sheet and one silica tetrahedron sheet in a 1 : 1 stoichiometric ratio, and it is available in abundance in China as well as other locations around the world. Halloysite has similar structure and composition as kaolinite, but the unit layers are separated by a monolayer of water molecules. The interlayer water is weakly held, so that halloysite-10 Å can readily transform to halloysite-7 Å. Halloysite nanotubes (HNTs) have large specific surface area, abundant hydroxyl group and nanotubular structure in the submicrometer range [22]. It is heartening to compare HNTs with other nano-sized material such as widely used carbon nanotubes (CNTs): HNTs are readily obtainable and much cheaper, and have some advantages in applications which require a biocompatible nanocontainer. More attractively, the unique tubular structure of HNTs resembles that of CNTs. Therefore, HNTs may have the potential to provide cheap and effective alternatives for dye removal [23-25].

Literature citations reveal that most clays previously used as adsorbents need to be modified by surface active agents, oxides etc., in order to enhance their adsorption capacity. However, these modifications of clays may complicate the operation and thus increase the costs. Therefore, a fine balance is needed between the effectiveness and costs. The starting premise of this work was to develop an efficient adsorbent based on halloysite for the removal of dyes by performing a cheaper and simple modification under "mild" operating conditions. Chemical activation can be selected and several prior works have been reported [11,26,27]. Acid activation, which has in the past been universally used in ore dressing process, is an important aspect for chemical activation. It can effectively remove salts and other acid dissolved impurities, and increase the number and activity of active groups such as hydroxyl, carboxyl on the ad-

†To whom correspondence should be addressed.
E-mail: zhangb@zzu.edu.cn

sorbent surface. Besides, acid activation is relatively easy to operate and low-budget compared with modification by surface active agents and oxides because acid is relatively inexpensive and recyclable.

Thus, the present study was devoted to producing chemically activated halloysite nanotubes (C-HNTs) and testing their ability to remove a model dye, methylene blue (MB), which has been extensively used for dyeing leather, calico and cotton etc., indicating oxidation-reduction and tissue staining. Our purpose was to evaluate the adsorption capacity of C-HNTs and examine the possibility of practically using C-HNTs to remove MB. C-HNTs were obtained by treatment of raw halloysite nanotubes (HNTs) with hydrochloric acid (HCl) followed by sodium chloride (NaCl) at room temperature. Then C-HNTs were carefully characterized and their adsorption properties were studied using batch method. Parameters affecting the adsorption process including adsorbent dose, pH, initial MB concentration, temperature, and contact time were investigated. In addition, isotherms, kinetics and thermodynamics were also studied. The results indicated that C-HNTs can be used as an economic and efficient adsorbent for removal of MB from wastewater and were valuable for further application of C-HNTs in dye removal.

MATERIALS AND METHODS

1. Preparation of C-HNTs

The preparation of C-HNTs as adsorbent was performed as follows: (i) Halloysite clay from Henan Province (China) was milled and sieved followed by oven dried at 383 K for 24 h in order to obtain raw HNTs. (ii) 10 g of raw HNTs was slowly added to 100 mL 1 mol·L^{-1} of HCl with magnetically stirring for 12 h, and then left to rest at 298 K for 24 h. Afterward, the sample solution was then filtered off using a centrifugal separator and washed sequentially with distilled water three times to remove the ions and other residues. The resulting product was finally dried at 378 K for 12 h. (iii) The product was suspended in 100 mL 1 mol·L^{-1} of NaCl aqueous solution and agitated for 2 h at 323 K, and then left to rest at room temperature for 12 h. The suspension was filtered and the solid material was washed repeatedly with distilled water three times and finally dried at 373 K for 12 h. (iv) The obtained product was ground and stored in a desiccator prior to the physical and chemical characterizations.

2. Preparation of MB Solution

MB (CI: 52015; chemical formula: $C_{16}H_{18}N_3SCl{\cdot}3H_2O$; molecular weight: 373.90) was supplied by Merck, without further purification prior to use. The maximum wavelength of MB is 668 nm, which does not vary with solution pH in the range from pH 2 to pH 10. A stock solution (1,000 mg·L^{-1}) was prepared by dissolving MB in distilled water; desired concentrations were obtained when needed by diluting the stock solution with distilled water.

3. Instrumentation and Characterization

X-ray powder diffraction (XRD) pattern was obtained with a Philips X Pert-Pro diffractometer with CuKα (λ=0.154 nm) radiation operating at 35 kV and 25 mA and a step width of 0.04°. Fourier transformed infrared spectroscopy (FTIR) was recorded on a Nicolet Nexus 470 FTIR spectrometer in the range 400-4,000 cm^{-1}. The size and morphology of the product was characterized with a FEITECNAlG2 transmission electron microscope (TEM). BET surface area was calculated from nitrogen adsorption-desorption measurements at 77 K by using a Quantachrome NOVA 4200e instrument. The zeta potential of C-HNTs suspensions was measured with a Malvern Zetasizer Nano ZS in order to obtain the pH of zero point charge (pH_{zpc}) by plotting zeta potential versus pH.

4. Adsorption Experiments

All the experiments were performed in a stopper conical flask containing 25 mL varying initial concentration of MB solutions and adsorbent dose. Then the samples were agitated on a thermostatted shaker with a shaking of 180 rpm at 298-318 K. The effect of adsorbent dose on the removal of MB was obtained by contacting 25 mL of MB solution of initial dye concentration of 100 mg·L^{-1} with different weighed amount (0.025-0.25 g) of C-HNTs. The system was maintained under shaking at 298 K for 4 h until adsorption reached equilibrium. The influence of pH on MB removal was studied by adjusting MB solutions (100 mg·L^{-1}) to different pH values (3.0-9.0) using a pH 211 Microprocessor pH Meter and agitating 25 mL of dye solution with 0.05 g adsorbent at 298 K for 4 h. The pH was adjusted using 0.1 mol·L^{-1} NaOH and 0.1 mol·L^{-1} HCl solutions. The effect of temperature and initial concentration was carried out in the 25 mL of dye solutions in different initial concentration ranging from 50 to 500 mg·L^{-1} with 0.05 g of adsorbent under 298, 308 and 318 K for 4 h, respectively. The effect of contact time was obtained with 25 mL of dye solution containing 0.05 g adsorbent at different initial dye concentration ranging from 50 to 300 mg·L^{-1} at 298 K for 4 h.

The equilibrium concentrations of MB were determined by analyzing samples after centrifugation at 3,000 rpm in the laboratory with the colorimetric method. The concentration of MB in each aqueous solution was measured on ultraviolet-visible spectrophotometry (UV-Vis, Shimadzu, Japan) by measuring absorbance at λ_{max} of 668 nm. The removal efficiency (R, %), the amount of MB adsorbed at time t (q_t, mg·g^{-1}) and at equilibrium (q_e, mg·g^{-1}) was calculated by using the following equations, respectively.

$$R=100(C_0-C_e)/C_0 \quad (1)$$

$$q_t=(C_0-C_t)V/m \quad (2)$$

$$q_e=(C_0-C_e)V/m \quad (3)$$

where C_0, C_t and C_e (mg·L^{-1}) are the initial, t time and equilibrium concentrations of MB solution, respectively; V (L) is the volume of MB solution and m (g) is the weight of C-HNTs.

To quantitatively compare the applicability of each model, a data analysis was carried out using correlation analysis employing least-square method, and the average relative standard error (ARSE, %) is calculated as follows:

$$ARSE=100\times\sqrt{\sum_{i=1}^{n}[(q_{e,exp}-q_{e,cal})/q_{e,exp}]^2/(n-1)} \quad (4)$$

where n is the number of data points.

RESULTS AND DISCUSSION

1. Characterization of C-HNTs

The XRD pattern of C-HNTs is shown in Fig. 1. It shows that the diffraction peaks can be indexed to the hexagonal structured $Al_2Si_2O_5(OH)_4$, which is in agreement with the reported values of Halloysite-7 Å with the lattice constants a=5.13, c=7.16 (JCPDS

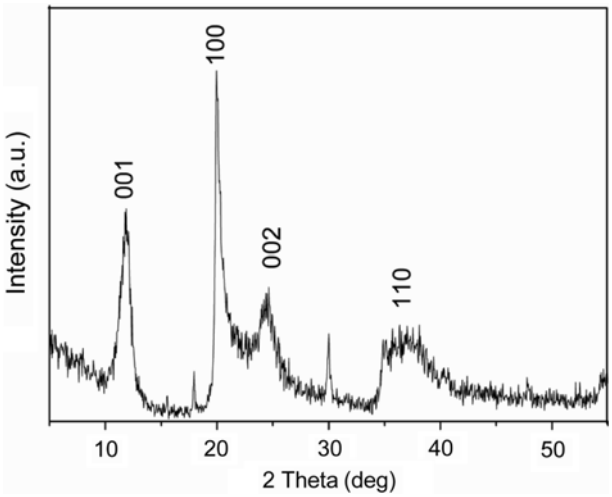

Fig. 1. The XRD pattern of C-HNTs.

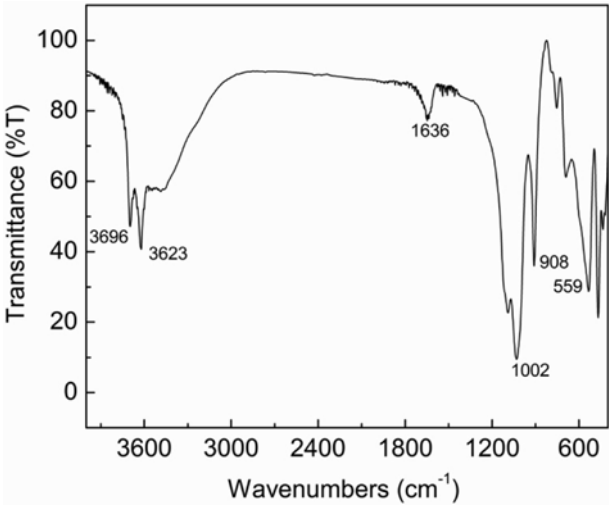

Fig. 2. The FTIR spectra of C-HNTs.

Card No. 29-1487). The significant broadening of the diffraction peaks is ascribed to the very small crystallite size.

The FTIR spectrum of C-HNTs is depicted in Fig. 2. The peaks at 3,696 and 3,623 cm^{-1} are attributed to the stretching vibrations of inner-surface hydroxyl groups, whose deformation vibration is at 908 cm^{-1}. The band at 1,002 cm^{-1} is caused by the stretching vibrations of Si-O-Si. The 559 cm^{-1} peak is assigned to deformation vibration of Al-O-Si. Interlayer water is indicated by the deformation vibration at 1,636 cm^{-1}. C-HNTs have a large number of hydroxyl group which is the main functional group interacting with MB.

The TEM image of C-HNTs is shown in Fig. 3. C-HNTs have a cylindrical shape and contain a transparent central area that runs longitudinally along the cylinder, indicating that the nanotubular particles are hollow and open-ended. The typical morphological parameters of C-HNTs, obtained mainly according to the scale computation of TEM image, are as follows: the average length is 0.5-1 μm; the external diameter is in the range of 20-50 nm; and the inner diameter is 10-30 nm. Note that the accuracy of these parameters is limited by the morphology and number of particles observed in the TEM images. The large and smooth unhindered pores can

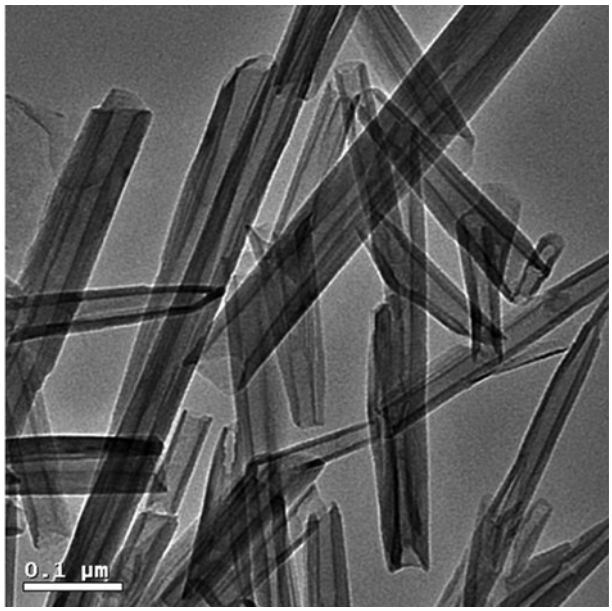

Fig. 3. The TEM micrograph of C-HNTs.

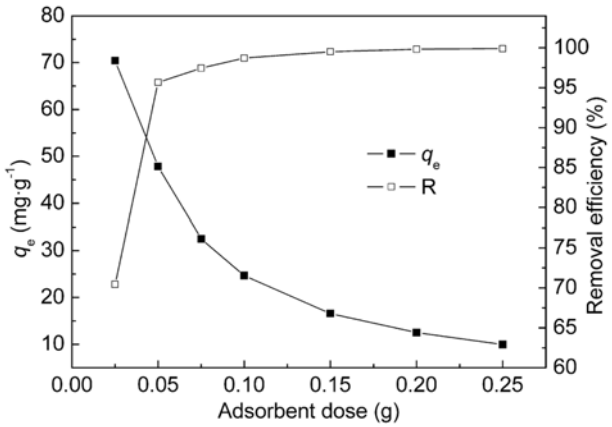

Fig. 4. Effect of adsorbent dose for MB adsorption onto C-HNTs at 298 K.

provide sufficient space for potential adsorption of MB. The specific surface area of C-HNTs calculated was 68.38 $m^2 \cdot g^{-1}$. The relative large specific surface area and pores could provide more active sites that could interact with MB cations.

The pH_{zpc} value of C-HNTs was found to be 2.2. The surface charge of C-HNTs was slightly positive at very low pH (lower than 2.2), and would be negative over a wide range of pH values (higher than 2.2). As a result, C-HNTs tend to readily bind cations in aqueous solutions.

2. Effect of Adsorbent Dose

To optimize the adsorbent dose for the removal of MB from aqueous solutions, adsorption was carried out with different adsorbent dose in 25 mL 100 $mg \cdot L^{-1}$ MB aqueous solution at 298 K for 4 h. The results (Fig. 4) show an increase in removal efficiency from 70.45% to 99.90% with the increase in dosage of adsorbent from 0.025 to 0.25 g. As the adsorbent dose increases, the adsorbent sites available for the dye cations also increase, and consequently better adsorption takes place. However, the adsorption capacity decreases

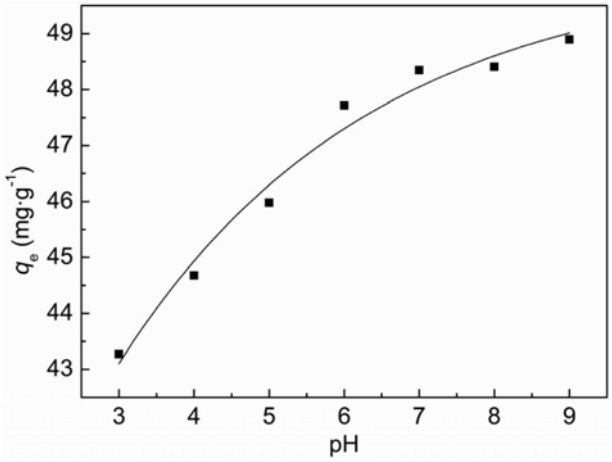

Fig. 5. Effect of pH for MB adsorption onto C-HNTs at 298 K.

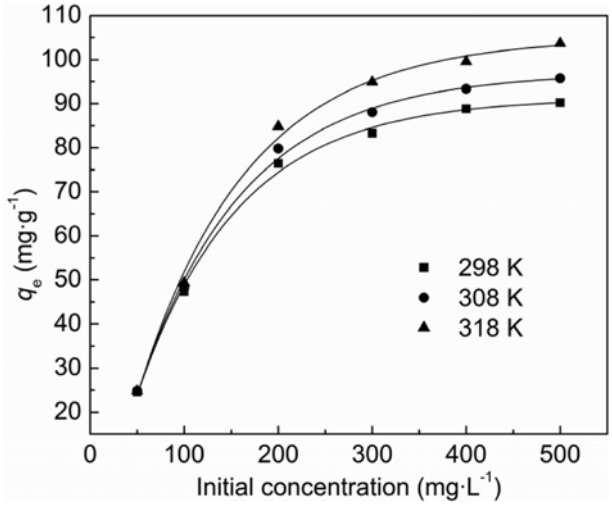

Fig. 6. Effect of initial MB concentration and temperature for MB adsorption onto C-HNTs.

from 70.45 to 9.99 mg·g^{-1} as the adsorbent dose increases from 0.025 to 0.25 g. Thus, the optimum amount of adsorbent dose was chosen as 0.05 g. In this case the adsorption is efficient (removal efficiency higher than 95%) without sacrificing unnecessary use of excess adsorbent.

3. Effect of pH

Experiments were carried out using various pH solutions from 3.0 to 9.0 for 25 mL 100 mg·L^{-1} MB concentration at 298 K for 4 h. Final pH when the adsorption was completed was also measured and the variation was all within 1 pH unit. The effect of pH on the adsorption of MB at equilibrium is shown in Fig. 5. The q_e is found to increase from 43.27 to 48.89 mg·g^{-1} with increasing pH from pH 3.0 to pH 9.0. The strong dependence of adsorption capacity on pH could be attributed to the fact that the surface charge of C-HNTs is greatly affected by solution pH. The pH_{zpc} of C-HNTs was found to be 2.2. The surface of C-HNTs is positively charged below pH 2.2, while it acquires a negative charge above this pH. Besides, the zeta potential of C-HNTs is more negatively charged with increase in pH in the range pH 3.0 to pH 9.0. MB produces molecular cations in aqueous solution. Therefore, increasing electrostatic attractions between negatively charged adsorption sites and positively charged MB cations causes an increase in MB removal. Lower adsorption at lower pH is due to the presence of excess of H^+ ions competing with the dye cations for adsorption sites. As the initial pH of MB solution without adjustment is approximately 7.0 in this study, the pH 7.0 was chosen in the next experimental solution.

4. Effect of Initial Concentration and Temperature

Batch adsorption studies were carried out with initial MB concentrations ranging from 50 to 500 mg·L^{-1} at 298-318 K for 4 h. Fig. 6 shows the adsorption uptake versus the initial MB concentrations at various temperatures. The amount of dye adsorbed increased with increase in concentration and temperature. The amount of dye removal increased from 24.79 to 103.68 mg·g^{-1} with the increase in dye concentration from 50 to 500 mg·L^{-1} at 318 K. It is clear that the removal of the dye depends on the concentration of the dye because the initial dye concentration provides the necessary driving force to overcome the resistance to the mass transfer of MB between the aqueous and solid phases. Temperature has an important effect on the adsorption process. The equilibrium capacity of the adsorbent for MB increases from 90.25 mg·g^{-1} at 298 K to 103.68 mg·g^{-1} at 318 K. As the temperature increases, the rate of diffusion of MB molecules across the external boundary layer and internal pores of the adsorbent particle increases. The fact that adsorption capacity of MB onto C-HNTs increases with increase in temperature indicates the process is endothermic in nature.

5. Effect of Contact Time

The adsorption data for the uptake of MB versus contact time at different initial dye concentration ranging from 50 to 300 mg·L^{-1} are presented in Fig. 7. It is observed that a large amount of MB was rapidly removed by C-HNTs during the first 30 min. After then, rate of removal of dyes slowed down gradually until the equilibrium state. The rapid adsorption observed during the first 30 min was probably due to the abundant availability of active sites on the C-HNTs surface, and with the gradual occupancy of these sites, the adsorption became less efficient. The equilibrium time is independent of initial MB concentration. But in the first 30 min, the initial rate of adsorption was greater for higher initial MB concentration.

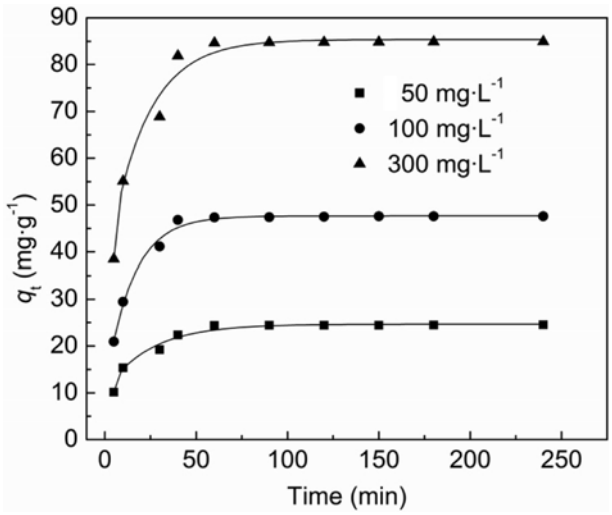

Fig. 7. Effect of contact time for MB adsorption onto C-HNTs.

On changing the initial concentration of MB from 50 to 300 mg·L^{-1}, the amount adsorbed increased from 24.53 to 84.93 mg·g^{-1}. This can be attributed to greater driving force, resulted from greater concentration gradient between MB in solution and MB on the adsorbent surface at higher initial dye concentration.

6. Adsorption Isotherms

Equilibrium data, commonly known as adsorption isotherms, are of great importance in the design of adsorption systems. These data provide information on the capacity of the adsorbent or the amount required for removing a unit mass of pollutant under the system conditions. In the present study, the Langmuir and Freundlich are selected.

The Langmuir equation assumes that there is no interaction between the adsorbate molecules and that the adsorption is localized in a monolayer. It is then assumed that once a dye molecule occupies a site, no further adsorption can take place at that site. The well known expression of the Langmuir model is given as:

$$C_e/q_e=1/q_{max}K_L+C_e/q_{max} \quad (5)$$

where q_e (mg·g^{-1}) s the equilibrium amount of MB adsorption by C-HNTs, C_e (mg·L^{-1}) is the equilibrium MB concentration in the solution, q_{max} (mg·g^{-1}) is the maximum uptake of MB and K_L (L·mg^{-1}) is the Langmuir constant. q_{max} and K_L constants are calculated from the slope and intercept of the plot of C_e/q_e versus C_e and are given in Table 1, respectively. To determine if the adsorption process is favorable or unfavorable, a dimensionless constant separation factor or equilibrium parameter R_L, is defined according to the following equation:

$$R_L=1/(1+K_LC_0) \quad (6)$$

where K_L (L·mg^{-1}) is the Langmuir constant and C_0 (mg·L^{-1}) is the initial MB concentration. The R_L value indicates the adsorption process is irreversible when R_L is 0; favorable when R_L is between 0 and 1; linear when R_L is 1; and unfavorable when R_L is greater than 1.

The Freundlich isotherm is the earliest known relationship describing the adsorption equation. This fairly satisfactory empirical isotherm can be used for nonideal adsorption that involves heterogeneous surface energy systems. The Freundlich isotherm is commonly given as:

$$\log q_e=\log K_F+\log C_e/n \quad (7)$$

where K_F ($mg^{1-1/n}\cdot L^{1/n}\cdot g^{-1}$) and 1/n are Freundlich constants related to adsorption capacity and adsorption intensity, respectively. Higher value for K_F indicates higher affinity for adsorbate and the values of the empirical parameter 1/n lie between $0.1<1/n<1$, indicating favorable adsorption. K_F and 1/n can be determined from the linear plot of $\log q_e$ versus $\log C_e$, respectively.

Parameters and correlation coefficients obtained from Langmuir and Freundlich models are summarized in Table 1. It was found that the fitting to the Langmuir model gave slightly higher values of correlation coefficients (r^2) than those for the Freundlich model at the temperature investigated. Furthermore, the values of ARSE (%) for the Langmuir model were all lower than those for Freundlich model. The above results showed that the Langmuir model is better than Freundlich model in describing the behavior of MB adsorption onto C-HNTs, implying that the adsorption process could be a homogeneous distribution onto C-HNTs surface. Both the two isotherm models at a temperature of 298 K are illustrated in Fig. 8.

From Table 1, the highest q_{max} value was found as 103.63 mg·g^{-1}

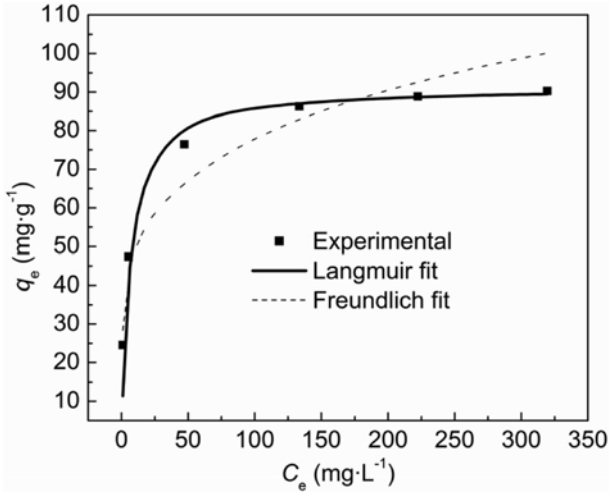

Fig. 8. Comparison of different isotherm models for MB adsorption onto C-HNTs at 298 K.

Table 1. Isotherm constants for MB adsorption onto C-HNTs

Isotherm models	Temperature (K)		
	298	308	318
Langmuir			
q_e (mg·g^{-1})	90.25	95.71	103.68
q_{max} (mg·g^{-1})	91.32	96.34	103.63
K_L (L·mg^{-1})	0.1508	0.1758	0.2167
R_L	0.0131-0.117	0.0112-0.102	0.00915-0.0845
r^2	0.9996	0.9995	0.9994
ARSE (%)	2.51	3.83	3.79
Freundlich			
K_F ($mg^{1-1/n}\cdot L^{1/n}\cdot g^{-1}$)	28.71	32.88	37.30
1/n	0.2167	0.2029	0.1963
r^2	0.9720	0.9805	0.9547
ARSE (%)	12.1	10.4	17.0

Table 2. Comparison of adsorption capacity of MB onto various adsorbents

Adsorbents	Temperature (K)	Capacity (mg·g^{-1})	References
C-HNTs	308	95.7	This Study
Flyash	303	3.1	[28]
Coir pith carbon	298	5.9	[29]
Coal fly ash	295	7.1	[30]
Neem leaf powder	300	8.8	[31]
Kaolinite	300	14.0	[16]
Coconut shell activated carbon	303	19.6	[32]
MCM-41	303	56.1	[33]
Peanut hull	293	68.0	[8]
Spent activated clay	298	91.2	[34]
Sewage sludge activated carbon	298	115.1	[6]
H_3PO_4 activated carbon	298	315.9	[35]

at 318 K from the Langmuir model. The R_L values ranged between 0.00915 and 0.117, which confirmed the adsorption process is favorable. A comparison of MB adsorption capacity of various adsorbents is presented in Table 2. It is observed that our result is similar to spent activated clay and sewage sludge, while higher than peanut hull, natural zeolite, neem leaf powder and coir pith carbon, etc., which confirmed that C-HNTs has comparable higher adsorption capacity for removing MB. Variation in MB adsorption capacity is mainly attributed to the difference in the property of adsorbent and experimental condition involved.

r^2 for Freundlich are all higher than 0.95, to a certain extent indicating the model is suitable to describe the adsorption process. The Freundlich model constants, K_F and 1/n, can also give information about the adsorption process. KF increases with increasing temperature in the range 298 K to 318 K, indicating higher affinity of C-HNTs for adsorbate, which can be demonstrated by the increase of adsorption capacity. The values of 1/n 0.2167, 0.2029 and 0.1963 at 298, 308 and 318 K are all smaller than 1, representing the favorable removal conditions.

7. Adsorption Kinetics Modeling and Mechanism

To examine the mechanism of adsorption process such as mass transfer and chemical reaction, a suitable kinetic model is needed to analyze the rate data. The following kinetic models were adopted to examine the experimental data: (i) Pseudo-first-order equation; (ii) Pseudo-second-order equation; (iii) Elovich equation; (iv) Intra-particle diffusion equation.

7-1. The Pseudo-first-order Equation

The pseudo-first-order equation can be expressed as follows:

$$\log(q_e - q_t) = \log q_e - k_1 t/2.303 \quad (8)$$

where q_e and q_t ($mg \cdot g^{-1}$) are the MB adsorption capacity at equilibrium and at time t (min), respectively, and k_1 (min^{-1}) is the rate constant of the pseudo-first-order.

The parameters k_1 and q_e could be calculated from the slope and intercept of the plots of $\log(q_e - q_t)$ versus t and are given in Table 3. The values of the correlation coefficient r_1^2 obtained at all the studied concentrations are low, in the range 0.7505-0.7885. Furthermore, the experimental values of $q_{e,exp}$ ($mg \cdot g^{-1}$) are far from the calculated $q_{e,cal}$ ($mg \cdot g^{-1}$) and ARSE (%) are too high. These suggest that the pseudo-first-order kinetic model is not suitable to describe the adsorption process.

7-2. The Pseudo-second-order Equation

The linear pseudo-second-order equation is given by:

$$t/q_t = 1/k_2 q_e^2 + t/q_e \quad (9)$$

where k_2 ($g \cdot mg^{-1} \cdot min^{-1}$) is the rate constant of the pseudo-second-order. The q_e and k_2 values can be obtained from the slope and intercept of plots of t/q_t versus t. Applying the pseudo-second-order model it is more likely to predict the behavior over the whole range of adsorption, while chemical reaction seems significant in the rate-controlling step.

The good linear plots of t/q_t versus t at different concentrations with the highest correlation coefficients r_2^2 (higher than 0.999) and the lower ARSE (%) suggest that adsorption of MB onto C-HNTs follows the pseudo-second-order kinetic model. Besides, the calculated data ($q_{e,cal}$) agree well with the experimental data ($q_{e,exp}$). The parameters are listed in Table 3. The same conclusion was found in the literature on the adsorption of MB by montmorillonite clay [36] and sonicated sepiolite [37].

7-3. The Elovich Equation

The Elovich equation is generally expressed as:

$$q_t = \ln(\alpha\beta)/\beta + \ln t/\beta \quad (10)$$

where α is the initial adsorption rate constant ($mg \cdot g^{-1} \cdot min^{-1}$), and β is the desorption constant ($g \cdot mg^{-1}$). The β and α value can be obtained from the slope and intercept of plots of q_t versus lnt and are given in Table 3.

Compared with pseudo-second-order model, the values of the correlation coefficient r_3^2 obtained at all the studied concentrations are lower, in the range 0.9121-0.9393, while the ARSE (%) values are higher, indicating the Elovich equation cannot be used to describe the kinetics in this study.

7-4. The Intra-particle Diffusion Equation

Because the three models above cannot identify the diffusion mechanism during the adsorption process, the experimental data are tested by the intra-particle diffusion model, which can be expressed by following equation:

$$q_t = k_p t^{1/2} + C \quad (11)$$

where q_t ($mg \cdot g^{-1}$) is the amount of MB adsorbed at time t (min), k_p ($mg \cdot g^{-1} \cdot min^{-1/2}$) is the Intra-particle diffusion rate constant and C is the intercept.

The rate constants k_p, C, r_4^2 are shown in Table 3. The correlation coefficients r_4^2 for the intra-particle diffusion model are between 0.9868 and 0.9922, which are slightly lower than those for pseudo-second-order equation. However, the ARSE (%) is lower than that for pseudo-second-order equation. These indicate that the adsorption of MB onto C-HNTs may be followed by the intra-particle dif-

Table 3. Kinetic parameters for MB adsorption onto C-HNTs

Kinetic models	Dye concentration ($mg \cdot L^{-1}$)		
	50	100	300
$q_{e,exp}$ ($mg \cdot g^{-1}$)	24.53	47.59	84.93
Pseudo-first-order			
$q_{e,cal}$ ($mg \cdot g^{-1}$)	6.33	8.12	14.40
k_1 (min^{-1})	0.01078	0.01248	0.01560
r_1^2	0.7885	0.7505	0.7885
ARSE (%)	90.92	95.17	94.16
Pseudo-second-order			
$q_{e,cal}$ ($mg \cdot g^{-1}$)	25.34	48.80	87.26
k_2 ($g \cdot mg^{-1} \cdot min^{-1}$)	0.00673	0.00474	0.00246
r_2^2	0.9996	0.9997	0.9997
ARSE (%)	6.53	10.19	7.49
Elovich			
α ($mg \cdot g^{-1} \cdot min^{-1}$)	22.15	63.45	124.30
β ($g \cdot mg^{-1}$)	0.271	0.148	0.0844
r_3^2	0.9393	0.9121	0.9246
ARSE (%)	10.10	11.11	9.87
Intra-particle diffusion			
k_p ($mg \cdot g^{-1} \cdot min^{-1/2}$)	5.46	11.12	18.44
r_4^2	0.9893	0.9922	0.9868
ARSE (%)	3.36	2.18	3.13

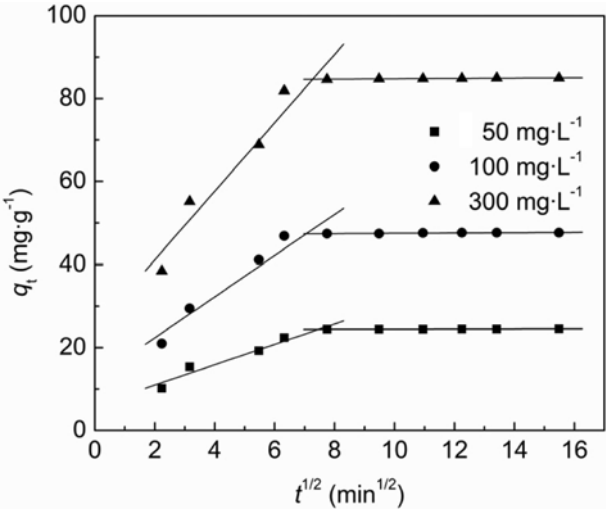

Fig. 9. Plots of Intra-particle diffusion equation for the adsorption of MB onto C-HNTs at different initial concentrations.

fusion model.

The intra-particle diffusion model presents multi-linearity (Fig. 9), indicating that two steps take place. The sharper first-stage portion is attributed to the diffusion of adsorbate though the solution to the external surface of adsorbent or the boundary layer diffusion of solute molecules. The second portion describes the gradual adsorption stage until equilibrium is reached, where intra-particle diffusion is rate-limiting. During these two stages, MB cations are slowly transported via intra-particle diffusion in the particles and are finally retained in the micropores. In general, the slope of the line of the first stage is called the intra-particle diffusion rate constant, which is listed in Table 3. In Fig. 9, the linear portion of the first stage does not pass though the origin, indicating there is a boundary layer resistance between adsorbent and adsorbate. The deviation from the origin is proportional to the boundary layer thickness. It is observed that values of k_p increase from 5.46 to 18.44 mg·g^{-1}·min$^{-1/2}$ when the initial MB concentrations increase from 50 to 300 mg·L^{-1}.

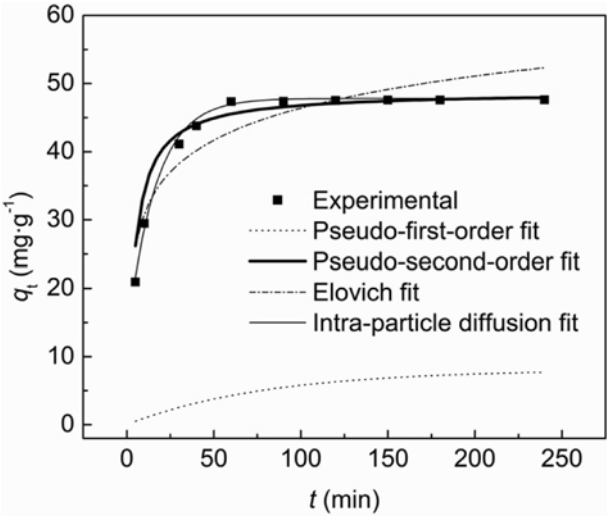

Fig. 10. Comparison of the measured and modeled time profiles for the adsorption of MB onto C-HNTs at 100 mg·L^{-1}.

A comparison of calculated and measured results for 100 mg·L^{-1} MB concentration is shown in Fig. 10. The pseudo-second-order and intra-particle diffusion model fit the experimental data very well, whereas the Elovich and pseudo-first-order do not give good fits to the experimental data for the adsorption of MB onto C-HNTs. The applicability of the four models approximately follows the order: Pseudo-second-order, Intra-particle diffusion>Elovich>Pseudo-first-order.

In the present study, we propose that ion exchange is the primary mechanism for adsorption of MB cations onto the surface of C-HNTs. FTIR analysis indicates that the surface of C-HNTs bears abundant hydroxyl groups, which can be used as active adsorption sites. Most of the hydroxyl groups could be transformed to the form of O-Na after saturation of sodium chloride, which can further increase their activity due to the weaker binding of O-Na in aqueous solutions. A possible mechanism of ion exchange could be considered as MB cation attaching itself to O-Na/H, forming O-MB compounds and releasing Na^+ or proton into the solution.

Besides, chemical interaction and electrostatic attraction between MB cations and O-Na/H on the surface may be additional contributive factors to the overall adsorption. The effect of pH on the adsorption process may confirm this. At lower pH, large amounts of hydroxyl groups exist in the form of Si (Al)-O-H due to the competitive adsorption of proton, which inhibits the interaction with MB^+. As pH increases, hydroxyl groups tend to exist in the negatively charged form Si (Al)-O^- and the interaction between Si (Al)-O^- and MB^+ becomes favorable. As a result, adsorption capacity of MB onto C-HNTs increases with increasing pH.

8. Thermodynamic Parameters

To gain an insight into the mechanism involved in the adsorption process, thermodynamic parameters for the present system are calculated. The adsorption free energy (ΔG^0), adsorption enthalpy (ΔH^0) and adsorption entropy (ΔS^0) at different temperatures (298, 308 and 318 K) are calculated using the following equations:

$$\Delta G^0 = -R_{gas} T \ln K_L \quad (12)$$

$$\Delta G^0 = \Delta H^0 - T\Delta S^0 \quad (13)$$

where K_L (L·mg^{-1}) is the Langmuir constant, R_{gas} (8.314 J·mol^{-1}·K^{-1}) is the universal gas constant and T (K) is the solution temperature. ΔH^0 and ΔS^0 are calculated from the intercept and slope of linear plot of ΔG^0 versus T. The values of ΔG^0, ΔH^0 and ΔS^0 parameters are summarized in Table 4.

Changes in the free energy ΔG^0 have negative values: –27.10, –28.41 and –29.88 kJ·mol^{-1} at 298, 308 and 318 K, respectively. These results indicate that MB adsorption by C-HNTs is spontaneous and has physical characteristics. The decrease in ΔG^0 value with increasing temperature reveals that adsorption of MB onto C-HNTs becomes more favorable at higher temperature. Change in the en-

Table 4. Thermodynamic parameters for MB adsorption onto C-HNTs

Temperature (K)	298	308	318
ΔG^0 (kJ·mol^{-1})	−27.10	−28.41	−29.88
ΔH^0 (kJ·mol^{-1})		14.65	
ΔS^0 (kJ·mol^{-1}·K^{-1})		0.14	

thalpy ΔH^0 value is 14.65 kJ·mol^{-1}, indicating that MB adsorption is an endothermic process. The positive value of the entropy change ΔS^0 (0.14 kJ·mol^{-1}·K^{-1}) suggests that randomness increases during the removal of MB on C-HNTs.

CONCLUSIONS

C-HNTs were obtained by treatment of raw HNTs with HCl followed by NaCl without heating or providing any other special condition, leading to a low-cost adsorbent with good affinity for positively charged species. The obtained material was characterized and used for MB dye removal from aqueous solution. The adsorption capacity increased with increasing pH, initial MB concentration and temperature.

The equilibrium data were best fitted by Langmuir adsorption isotherms. A maximum adsorption capacity of 103.63 mg·g^{-1} (temperature: 318 K; MB concentration: 500 mg·L^{-1}) was achieved.

The adsorption kinetics was well described by the pseudo-second-order and intra-particle diffusion model. Intra-particle diffusion analysis demonstrates that MB diffuses quickly among the particles at the beginning of the adsorption process, and then the diffusion slows down and stabilizes.

The adsorption mechanism of MB onto C-HNTs was explained by ion exchange of MB cation with sodium ion or proton generated from the adsorbent surface, which was considered to be the primary contribution. Chemical interaction and electrostatic attraction between MB cations and negatively charged binding sites were also contributive factors for adsorption.

Thermodynamic parameters suggest that the adsorption is spontaneous and endothermic.

In view of all these findings, it may be concluded that the developed adsorbent (C-HNTs) is effective and economical for the removal of MB from wastewater.

ACKNOWLEDGEMENTS

This work was supported by the National Natural Science Foundation of China (No. 20871105) and Henan Outstanding Youth Science Fund (No. 0612002400).

REFERENCES

1. V. K. Gupta and Suhas, *J. Environ. Manage.*, **90**, 2313 (2009).
2. H. S. Rai, M. S. Bhattacharyya, J. Singh, T. K. Bansal, P. Vats and U. C. Banerjee, *Crit. Rev. Environ. Sci. Technol.*, **35**, 219 (2005).
3. S. Artkla, K. Wantala, B. O. Srinameb, N. Grisdanurak, W. Klysubun and J. Wittayakun, *Korean J. Chem. Eng.*, **26**, 1556 (2009).
4. V. K. Gupta, R. Jain and S. Varshney, *J. Colloid Interf. Sci.*, **312**, 292 (2007).
5. Y. S. Al-Degs, M. A. M. Khraisheh, S. J. Allen and M. N. Ahmad, *J. Hazard. Mater.*, **165**, 944 (2009).
6. F. Rozada, L. F. Calvo, A. I. Garcia, J. Martin-Villacorta and M. Otero, *Bioresour. Technol.*, **87**, 221 (2003).
7. B. C. Kim, Y. H. Kim and T. Yamamoto, *Korean J. Chem. Eng.*, **25**, 1140 (2008).
8. R. M. Gong, Y. Z. Sun, J. Chen, H. J. Liu and C. Yang, *Dyes Pigm.*, **67**, 175 (2005).
9. J. Mao, S. W. Won, J. Min and Y. S. Yun, *Korean J. Chem. Eng.*, **25**, 1060 (2008).
10. R. W. Gaikwad and S. A. M. Kinldy, *Korean J. Chem. Eng.*, **26**, 102 (2009).
11. M. Hajjaji and H. El Arfaoui, *Appl. Clay Sci.*, **46**, 418 (2009).
12. V. K. Gupta, A. Mittal, A. Malviya and J. Mittal, *J. Colloid Interf. Sci.*, **335**, 24 (2009).
13. V. K. Gupta, R. Jain and S. Varshney, *J. Hazard. Mater.*, **142**, 443 (2009).
14. I. Ali and V. K. Gupta, *Nat. Protoc.*, **1**, 2661 (2006).
15. V. K. Gupta, I. Ali and V. K. Saini, *J. Colloid Interf. Sci.*, **315**, 87 (2007).
16. D. Ghosh and K. G. Bhattacharyya, *Appl. Clay Sci.*, **20**, 295 (2002).
17. E. Bulut, M. Ozacar and I. A. Sengil, *J. Hazard. Mater.*, **154**, 613 (2008).
18. M. Alkan, M. Dogan, Y. Turhan, O. Demirbas and P. Turan, *Chem. Eng. J.*, **139**, 213 (2009).
19. M. Dogan and M. Alkan, *Chemosphere*, **50**, 517 (2003).
20. V. K. Gupta, D. Mohan and V. K. Saini, *J. Colloid Interf. Sci.*, **298**, 79 (2006).
21. M. A. Al-Ghouti, M. A. M. Khraisheh, M. N. Ahmad and S. J. Allen, *J. Hazard. Mater.*, **146**, 316 (2007).
22. Y. M. Lvov, D. G. Shchukin, H. Mohwald and R. R. Price, *ACS Nano*, **2**, 814 (2008).
23. M. F. Zhao and P. Liu, *Micropor. Mesopor. Mater.*, **112**, 419 (2008).
24. P. Luo, Y. F. Zhao, B. Zhang, J. D. Liu, Y. Yang and J. F. Liu, *Water Res.*, **44**, 1489 (2010).
25. Y. F. Zhao, B. Zhang, X. Zhang, J. H. Wang, J. D. Liu and R. F. Chen, *J. Hazard. Mater.*, **178**, 658 (2010).
26. A. Aziz, M. S. Ouali, E. H. Elandaloussi, L. C. De Menorval and M. Lindheimer, *J. Hazard. Mater.*, **163**, 441 (2009).
27. D. Borah, S. Satokawa, S. Kato and T. Kojima, *J. Hazard. Mater.*, **162**, 1269 (2009).
28. V. V. B. Rao and S. R. M. Rao, *Chem. Eng. J.*, **116**, 77 (2006).
29. D. Kavitha and C. Namasivayam, *Bioresour. Technol.*, **98**, 14 (2007).
30. P. Janos, H. Buchtova and M. Ryznarova, *Water Res.*, **37**, 4938 (2003).
31. K. G. Bhattacharyya and A. Sharma, *Dyes Pigm.*, **65**, 51 (2005).
32. K. P. Singh, D. Mohan, S. Sinha, G. S. Tondon and D. Gosh, *Ind. Eng. Chem. Res.*, **42**, 1965 (2003).
33. P. Monash and G. Pugazhenthi, *Korean J. Chem. Eng.*, **27**, 1184 (2010).
34. C. H. Weng and Y. F. Pan, *J. Hazard. Mater.*, **144**, 355 (2007).
35. A. A. Attia, B. S. Girgis and N. A. Fathy, *Dyes Pigm.*, **76**, 282 (2008).
36. C. A. P. Almeida, N. A. Debacher, A. J. Downs, L. Cottet and C. A. D. Mello, *J. Colloid Interf. Sci.*, **332**, 46 (2009).
37. I. Kuncek and S. Sener, *Ultrason. Sonochem.*, **17**, 250 (2010).